

Gallium and Indium Arsanido Metalates: Compounds Derived from the Zinc Blende and Wurtzite Structure

Anahita Dashti-Mommertz and Bernhard Neumüller*

Marburg, Fachbereich Chemie der Universität

Received 19th January 1999.

Abstract. The reaction of InCl_3 with LiAs^tBu_2 in THF at -78°C gives the indium arsenide $\text{Cl}_2\text{InAs}^t\text{Bu}_2$ (**1**), which is dimer in solution and solid state. The corresponding reaction of InCl_3 with $\text{Li}_2\text{As}^t\text{Bu}$ leads to the metalate $[\text{Li}(\text{THF})_4]_2[(\text{InCl})_4(\text{InCl}_2)_2(\text{As}^t\text{Bu})_6]$ (**2**). The arsanido metalate $[\text{Li}(\text{THF})_4]_2[(\text{GaCl}_2)_6(\text{As}^t\text{Bu})_4] \cdot \text{THF}$ (**3** · THF) could be obtained by treatment of GaCl_3 with $\text{Li}_2\text{As}^t\text{Bu}$ in the molar ratio 6:4. A comparable reaction with TiCl_3 and LiAsR_2 or LiPR_2 , respectively, was not successful because of the oxidation potential of TiCl_3 . The reaction mixture of TiCl_3 and LiPPH_2 for example gives TiCl and $\text{Ph}_2\text{P}-\text{PPh}_2$ (**4**) as redox

products. The octaarsane $[\text{As}(\text{As}^t\text{Bu})_3]_2$ (**5**) can be obtained by the treatment of ${}^t\text{BuAs}(\text{SiMe}_3)_2$ with TiCl_3 in THF. **1–5** were characterized by NMR, IR and MS techniques. The X-ray analyses of **2** and **3** · THF show that **2** can be derived from the wurtzite structure while the zinc blende structure is the model for **3** with a adamantane-like dianion $[(\text{GaCl}_2)_6(\text{As}^t\text{Bu})_4]^{2-}$.

Keywords: Gallium arsanide; Indium arsanides; Lithium-organo arsanides; Crystal structures

Gallium- und Indium-Arsanidometallate: Verbindungen abgeleitet von der Zinkblende- und der Wurtzit-Struktur

Inhaltsübersicht. Die Reaktion von InCl_3 mit LiAs^tBu_2 in THF bei -78°C ergibt das Indiumarsanid $\text{Cl}_2\text{InAs}^t\text{Bu}_2$ (**1**), das als Dimer in Lösung und im Festkörper vorliegt. Die entsprechende Umsetzung von InCl_3 mit $\text{Li}_2\text{As}^t\text{Bu}$ führt zum Metallat $[\text{Li}(\text{THF})_4]_2[(\text{InCl})_4(\text{InCl}_2)_2(\text{As}^t\text{Bu})_6]$ (**2**). Das Arsanidometallat $[\text{Li}(\text{THF})_4]_2[(\text{GaCl}_2)_6(\text{As}^t\text{Bu})_4] \cdot \text{THF}$ (**3** · THF) kann bei der Behandlung von GaCl_3 mit $\text{Li}_2\text{As}^t\text{Bu}$ im molaren Verhältnis 6:4 erhalten werden. Eine vergleichbare Reaktion zwischen TiCl_3 und LiAsR_2 oder LiPR_2 führte aufgrund des Redoxpotentials des TiCl_3 nicht zum Er-

folg. Die Reaktionsmischung von TiCl_3 und LiPPH_2 z. B. ergibt TiCl und $\text{Ph}_2\text{P}-\text{PPh}_2$ (**4**) als Redoxprodukte. Das Oktaarsan $[\text{As}(\text{As}^t\text{Bu})_3]_2$ (**5**) wird bei der Umsetzung von ${}^t\text{BuAs}(\text{SiMe}_3)_2$ mit TiCl_3 in THF gebildet. **1–5** wurden durch NMR-, IR- und MS-Techniken sowie Kristallstrukturanalysen charakterisiert. Die Ergebnisse der Röntgenstrukturanalysen von **2** und **3** · THF zeigen, daß **2** von der Wurtzit-Struktur abgeleitet werden kann, während die Zinkblende-Struktur als Modell für **3** mit einem Adamantan-ähnlichen Dianion $[(\text{GaCl}_2)_6(\text{As}^t\text{Bu})_4]^{2-}$ dienen kann.

1 Introduction

Part of the recent efforts and developments in the organometal chemistry of group 13 metals is due to their possible use as single-source precursors for optoelectronic and semiconducting materials *via* MOCVD (metal-organic chemical vapor deposition) and MOVPE (metalorganic vapor phase epitaxy) methods [1–3]. At the same time the interest in new cyclic and cage compounds containing the atom combination group 13/group 15 starts to grow [4–17]. However, cages with group 13/As are still rare. Examples are the complexes $[(\{\text{Me}_3\text{Si}\}_2\text{CH})_2\text{Ga}]_3\text{Ga}_2(\text{AsPh}_2)(\text{AsPh})(\text{HAsPh})$ [18], $[\text{Li}(\text{DME})_3][\text{Li}(\text{DME})(\text{AlH}_2)_3\{\text{AsSiMe}_2(\text{CMe}_2)^t\text{Pr}\}]_3$ [19], $[\text{Li}_4(\text{OEt}_2)_8(\text{AlH})_4(\text{AsSi}^t\text{Pr}_3)_3]$ [20] and $[\text{HMER}]_6$

[$\text{M} = \text{Al, Ga; E} = \text{P, As; R} = \text{Si}^t\text{Pr}_3, \text{SiMe}_2(\text{CMe}_2)^t\text{Pr}$] [20]. A limiting factor in growing the size of such complexes is the bulk of the substituent on the metal and the pnictogen atom. For the build-up of a larger architecture, containing the group 13/group 15 element combination, a versatile substituent pattern on the metal would be one or more halogen atoms. Compounds of this type are known in gallium chemistry, e.g. $[\text{Br}_2\text{GaAs}(\text{CH}_2\text{SiMe}_3)_2]_3$ [21] and $[\text{I}_2\text{GaAs}(\text{SiMe}_3)_2]_2$ [22]. Subject of this study are the reactions of simple metal trihalides with mono- and dilithiumorgano pnictides in order to form metal inorganic ring and cage aggregates.

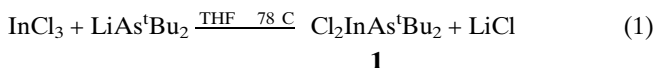
2 Results and Discussion

Our standard method to form M–E bonds ($\text{M} = \text{Al–In, E} = \text{N, P, As, S, Se, Te}$) is the treatment of the corresponding organometal halides R_2MX and RMX_2

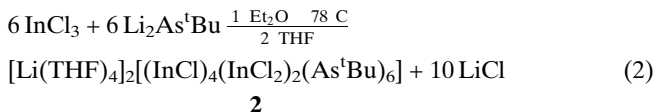
* Priv.-Doz. Dr. Bernhard Neumüller
Fachbereich Chemie der Universität
Hans-Meerwein-Strasse, D-35032 Marburg (Germany)
Fax: int-6421-288917
E-mail: neumueller@ax1502.chemie.uni-marburg.de

with a suitable lithium reagent LiER' or LiER'_2 [12, 13, 17, 23]. We intended to extend the metathesis procedure to the metal halides MX_3 of group 13. Our attempts to synthesize compounds such as $\text{X}_2\text{MPR}'_2$ by this method was not successful up to now.

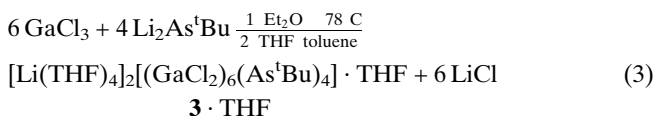
However, the reaction of InCl_3 with the diorganolithium arsanide LiAs^tBu_2 in THF at -78°C directly gives $\text{Cl}_2\text{InAs}^t\text{Bu}_2$ in good yield [Eq. (1)].



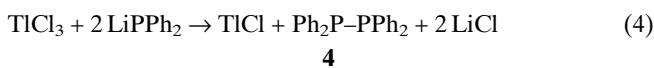
Keeping the same molar ratio of 1:1 of the educts InCl_3 and $\text{Li}_2\text{As}^t\text{Bu}$ at similar conditions the hexanuclear complex **2** was obtained [Eq. (2)].



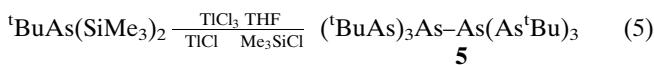
Although we performed the reaction of GaCl_3 and $\text{Li}_2\text{As}^t\text{Bu}$ also with a molar ratio of 1:1 only the compound **3** could be isolated. A clear increase of the yield was found after modifying the stoichiometry to 6:4 [Eq. (3)].



The mixtures containing lithium arsanides or phosphides and TlCl_3 very often gave precipitation of elemental thallium and LiCl . This was caused by the primary step, a reduction of TlCl_3 to TlCl [Eq. (4)]. The further reaction of TlCl with Li-reagents such as LiPR'_2 gave unstable Tl^I phosphides which undergo disproportionation to Tl^{III} species and Tl metal. The pnictide compounds were oxidized under E-E coupling in the primary step.



This oxidation reaction can be generalized. The disilylorganoarsane $^t\text{BuAs}(\text{SiMe}_3)_2$ is the starting compound for the formation of the bicyclic octaarsane $(^t\text{BuAs})_3\text{As}-\text{As}(\text{As}^t\text{Bu})_3$, first synthesized and structurally characterized by Fenske et al. [24] [Gl. (5)].



1–5 are air-sensitive colorless solids. The ^1H NMR spectra of **1** show only one signal for the ^tBu group at 1.21 ppm. Although it is possible to crystallize a dimeric and a trimeric modification, the predominating oligomer in solution is the dimer verified by cryoscopic measurements in benzene. VT-NMR investigations exhibit no evidence for other oligomers as could be shown for indium phosphides such as $^t\text{Pr}_2\text{InPPPh}_2$

and $(\text{PhCH}_2)_2\text{InPPPh}_2$ [17]. The resonances for the two ^tBu groups and one of the THF signals give a broad multiplet in the proton NMR spectrum of **2**. However, the ^{13}C NMR signals of the differing t-butyl substituents are separated (31.2, 34.9 ppm and 50.0, 51.3 ppm).

One can expect only one ^1H NMR signal for the CH_3 -groups in the dianion of **3**, which was detected at 1.92 ppm. The ^{31}P NMR resonance for the well-known compound **4** was found at -13.6 ppm [25, 26].

The two IR active In_2As_2 ring vibrations as well as the asymmetric and the symmetric InCl_2 vibrations are responsible for two broad absorptions at 250 and 327 cm^{-1} , respectively. The dianion in **2** causes a ν_{InCl} band for the ClInAs_3 moiety at 316 cm^{-1} and a ν_{InCl_2} band for the Cl_2InAs_2 moiety at 281 cm^{-1} . The absorption at 209 cm^{-1} is due to the asymmetric cage vibration $\nu_{\text{In}_6\text{As}_6}$. The dianion in **3** possesses nearly T_d -symmetry and shows the band for the asymmetric cage vibration $\nu_{\text{Ga}_6\text{As}_4}$ at 247 cm^{-1} . $\nu_{\text{as}}\text{GaCl}_2$ and $\nu_{\text{s}}\text{GaCl}_2$ were assigned to the signals at 331 and 296 cm^{-1} , respectively.

The heaviest mass particle was found for $m/z = 300$ $[(\text{ClInAs}_2)^+]$ in the EI mass spectra of **1**, **2** and **3** $[(\text{Ga}_2\text{As}(\text{C}_4\text{H}_9)_2)^+]$, while in the spectrum of **4** the M^+ peak could be detected at $m/z = 370$.

3 X-ray analyses of $[\mathbf{1}]_2$ –**4**

The structure of $[\text{Cl}_2\text{InAs}^t\text{Bu}_2]_2$ ($[\mathbf{1}]_2$) consists of centrosymmetric four-membered In_2As_2 rings with D_{2h} symmetry (Figure 1). The atoms In1, Cl1 and Cl2 lie on a mirror plane while a twofold axis is running through As1. The bond length In1–As1 of $265.2(1)\text{ pm}$ is short in comparison with other In_2As_2 compounds, probably due to the two electronegative Cl ligands [23]. Quite similar are the In–As distances in $[\text{Ph}_2\text{InAs}(\text{SiMe}_3)_2]_2$ with $265.7(3)$ – $267.9(2)\text{ pm}$ [24]. It is possible to obtain **1** also in a trimer modification by crystallization. Although the crystals of $[\mathbf{1}]_3$ were of no good quality we were able to solve the structure. Here, the basic structural motif was a distorted boat conformation. In general, the existence of two or more oligomers of one derivative $\text{R}_2\text{M-ER}'_2$ is not unusual [17].

The asterane-like centrosymmetric dianion $[(\text{InCl})_4(\text{InCl}_2)(\text{As}^t\text{Bu})_6]^{2-}$ contains two In–As six-membered rings (Figure 2) in a distorted boat conformation, which are connected by four In–As bonds to form two additional In–As four-membered rings. The In–As bonds involving In2 and As1 are significantly shorter (259 pm; mean value) than the corresponding values within the four-membered rings (267 pm). The reason is probably the μ^2 -bridging function of In2 and As1 concerning other In and As atoms, respectively. Typical distances in four-membered In–As heterocycles such as $[(\text{PhCH}_2)_2\text{InAs}^t\text{Bu}_2]_2$ [23] or

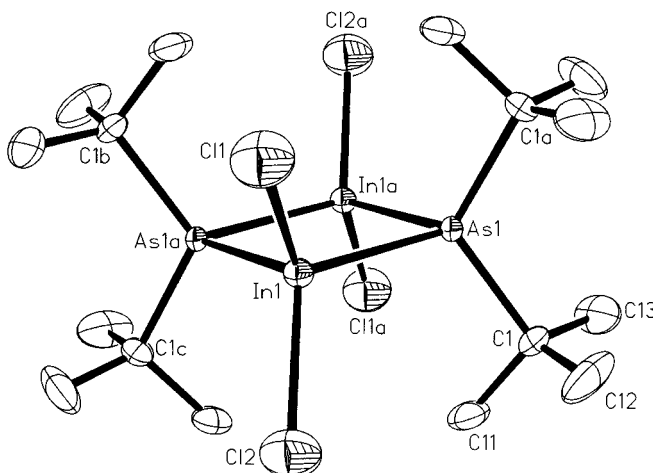


Fig. 1 Computer-generated plot of the dimeric unit $[1]_2$ (SHELXTL [45], ellipsoids at the 50% probability level, H atoms omitted for clarity).

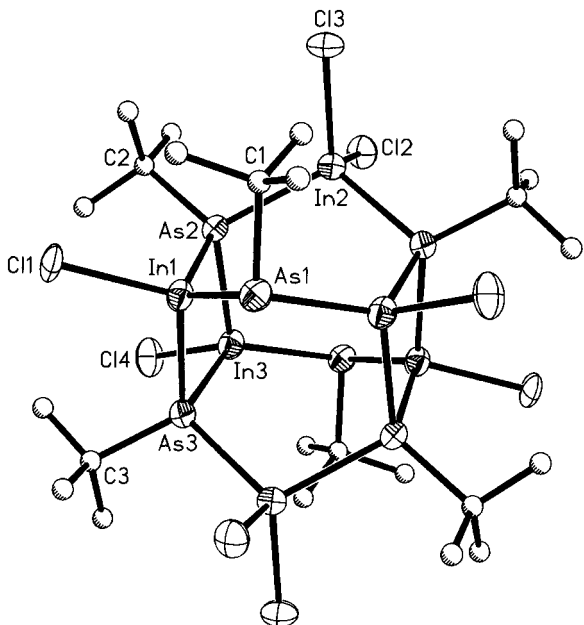


Fig. 2 Structure of the dianion $[(InCl)_4(InCl_2)_2(As^{tBu})_6]^{2-}$ in **2**.

$[Me_2InAsMe_2]_2$ [27] are 267–271 pm depending on the substituents. The largest deviation from a mean plane of the atoms In1, As2, In3 and As3 is 8 pm. With an average value of 249 pm the In–Cl bond lengths are somewhat longer than typical terminal In–Cl bonds containing indium centers with CN (coordination number) four [28]. Asterane structures in inorganic chemistry are known by the work of Fritz et al. [29]. The carbosilane $[Cl_2Si(CH)_2(SiCl)_2CH_2]_2$ is one of the examples; it was obtained by the pyrolysis of Me_2SiCl_2 [29 b, 29 c]. The asterane-like structure of the dianion in **2** can be derived from the wurtzite

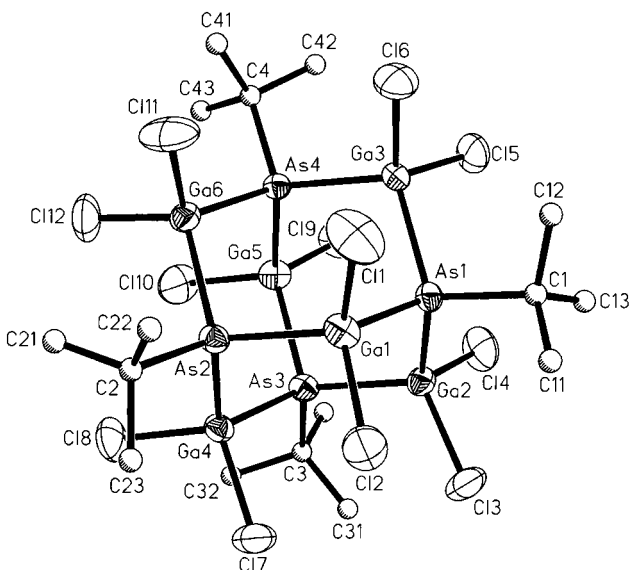
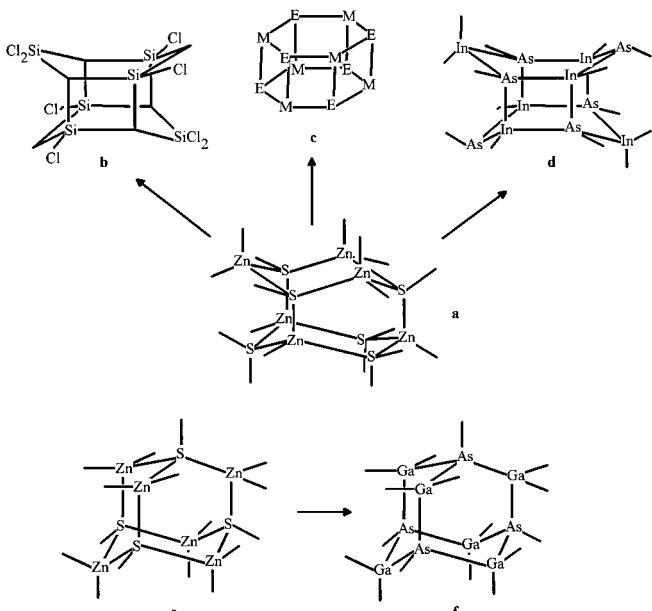


Fig. 3 Structure of the dianion $[(GaCl_2)_6(As^{tBu})_4]^{2-}$ in **3** · THF.



Scheme 1 a) Part of the wurtzite structure. b) Asterane structure of $[Cl_2Si(CH)_2(SiCl)_2CH_2]_2$ [29]. c) Basic skeleton in $[RMER']_6$ [20, 30–32]. d) In_6As_6 backbone of $[(InCl)_4(InCl_2)_2(As^{tBu})_6]^{2-}$ in **2**. e) Part of the zinc blende structure. f) Ga_6As_4 backbone of $[(GaCl_2)_6(As^{tBu})_4]^{2-}$ in **3** · THF.

structure (Scheme 1) as well as the recently published cage compounds $[HMER']_6$ [20], while the basic structural motif of the adamantane-like dianion of **3** · THF, $[(GaCl_2)_6(As^{tBu})_4]^{2-}$, is the zinc blende structure (Figure 3, Scheme 1). The reason for the domination of the wurtzite type in organometal chemistry is mainly

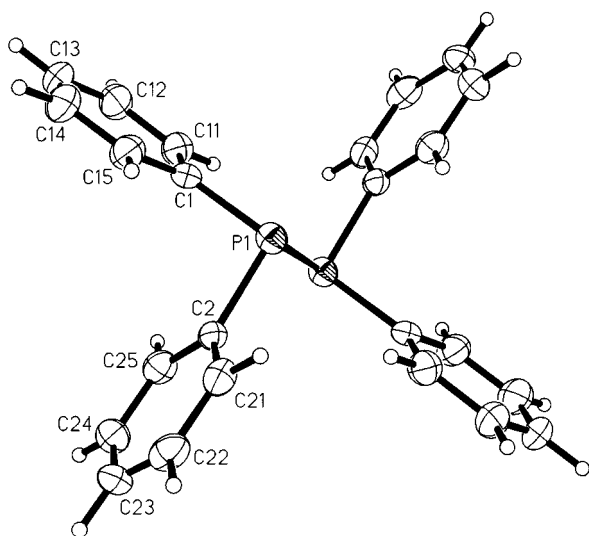


Fig. 4 Computer-generated plot of a molecule of $\text{Ph}_2\text{P}-\text{PPh}_2$.

due to the domination of the 1:1 composition in the derivatives [RM-ER'] shown e.g. in $[(\text{THF})\text{MgNPh}]_6$ [30], $[\text{LiNPPh}_3]_6$ [31] and $[\text{tBuGaS}]_6$ [32]. The adamantane-like type was found for example in $[(\text{IAI})_4(\text{S}_2)(\text{SMc})_4]$ [33]. The thermodynamic stable modification of GaAs and InAs at room temperature is in both cases the zinc blende structure [34].

Although $[(\text{GaCl}_2)_6(\text{As}^{\text{t}}\text{Bu})_4]^{2-}$ possesses only nearly T_d symmetry the Ga–As distances vary only between 243.3(1) and 244.7(1) pm. The values are even shorter than the bond lengths in gallium compounds with CN 3 at the gallium center such as ${}^{\text{t}}\text{Bu}_2\text{GaAs}^{\text{t}}\text{Bu}_2$ [246.6(3) pm] [35] and ${}^{\text{t}}\text{Bu}_2\text{GaAs}(\text{SiPh}_3)[\text{CH}(\text{SiMe}_3)_2]$ [245.8(1) pm] [36]. Comparable Ga–As atom distances were measured in $[(\{\{\text{Me}_3\text{Si}\}_2\text{CH}\}_2\text{Ga})_3\text{Ga}_2(\text{AsPh}_2) \cdot (\text{AsPh})(\text{HAsPh})]$ [245.0(1)–255.3(1) pm] [18], in $[\text{Br}(\{\text{Me}_3\text{SiCH}_2\}_2\text{As})\text{GaAs}(\text{CH}_2\text{SiMe}_3)_2]_2$ [terminal Ga–As bond: 243.7(1) pm] [37] and in $[\text{Br}_2\text{GaAs}(\text{CH}_2\text{SiMe}_3)_2]_3$ (245 pm) [21].

4 consists of centrosymmetric molecules with an *antiperiplanar* conformation (Figure 4). The two phenyl rings enclose an angle of 80°. The value of the P–P bond length of 221.7(1) pm is typical for diphosphanes [38]. The *antiperiplanar* conformation is also present in $\text{Me}_2\text{P}-\text{PM}_{\text{e}}$ (P–P: 221.2(1) pm) [38a] and in $\text{Mes}_2\text{P}-\text{PMes}_2$ with a long P–P distance of 226.0(1) ppm, caused by the bulk of the substituents [38b]. *Gauche* conformations have been observed in $(\text{C}_6\text{H}_{11})_2\text{P}-\text{P}(\text{C}_6\text{H}_{11})_2$ (P–P: 221.5(3) pm) [38c] and in $({}^{\text{t}}\text{Bu}_2\text{P})_2\text{P}-\text{P}({}^{\text{t}}\text{Bu}_2)_2$ (P–P average: 222 pm) [38d]. There is no short intermolecular contact in **4** ($\text{P}_1 \cdots \text{P}1\text{b}$: 406.7(1) pm) as it was observed for the higher homologues Sb and Bi [39]. This was expected on account of the detailed study of $\text{Me}_2\text{P}-\text{PM}_{\text{e}}$ (P–P: 381.3(1) pm) [38a].

Experimental Section

All experiments were carried out under an atmosphere of argon with Schlenk techniques. Purification and drying of the organic solvents were performed by standard methods [40]. MCl_3 ($\text{M} = \text{Ga}$ [41], In [41], Tl [42]), LiPPh_2 , $\text{LiAs}^{\text{t}}\text{Bu}_2$ and $\text{Li}_2\text{As}^{\text{t}}\text{Bu}$ [43] were prepared following literature procedures.

^1H , ^{13}C and ^{31}P NMR spectra were recorded on a Bruker AC-300 spectrometer (^1H : 300.133 MHz, ^{13}C : 75.469 MHz, ^{31}P : 202.456 MHz). TMS (^1H , ^{13}C) and 85% aqueous H_3PO_4 (^{31}P) were used as external standard, $\delta = 0.0$. IR spectra were obtained with a Bruker IFS-88 (nujol mulls, CsI discs for the range 4000–500 cm^{-1} ; polyethylen discs for the range 500–100 cm^{-1}). For the EI mass spectra a Varian CH 7a mass spectrometer (70 eV) was used. Melting points (uncorrected) were determined with a Dr. Tottoli (Büchi) melting-point apparatus in sealed capillaries under argon. The cryoscopic measurements were performed with a Normag molecular weight determination apparatus equipped with a Beckmann thermometer under argon.

Cl₂InAs^tBu₂ (1). To a suspension of 0.33 g (1.49 mmol) InCl_3 in 10 mL of THF 0.3 g (1.53 mmol) of $\text{LiAs}^{\text{t}}\text{Bu}_2$ in 10 mL of THF was added dropwise at –78 °C. The now orange solution was stirred for 3 h at –79 °C and 2 d at 20 °C. The solution was evaporated under vacuum and the residue was treated with 10 mL of toluene and filtered. The product precipitated at –25 °C.

Yield: 0.85 g (66%, based on InCl_3); m.p. 121 °C.

Elemental analysis: $\text{C}_{8}\text{H}_{18}\text{AsCl}_2\text{In}$ (374.88): calcd C 25.63, H 4.84, As 19.99, Cl 18.92; found C 25.81, H 4.90, As 20.13, Cl 18.62%.

^1H NMR (CD_3CN): 1.21 ppm (s, CCH_3).

^{13}C NMR (CD_3CN): 34.9 ppm (CCH_3), 55.0 ppm (CCH_3).

IR (Nujol, cm^{-1}): 2721 w, 1760 w, 1695 w, 1633 w, 1308 s, 1296 s, 1296 s, 1262 s, 1152 s, 1098 w, 1090 w, 1074 w, 1042 s, 1019 w, 966 w, 916 s, 887 s, 847 s, 801 m, 694 m, 673 m, 667 m, 644 w, 596 w, 590 w, 581 w, 558 w, 538 w, 527 w, 519 w, 494 w, 486 w, 477 w, 463 w, 430 w, 422 w, 415 w, 409 w, 327 s (νInCl_2), 250 m ($\nu\text{In}_2\text{As}_2$), 208 w, 185 w. EI MS (70 eV), m/z (rel. Int. in %): 300 (12) (ClInAs_2)⁺, 225 (2) (ClInAs)⁺, 190 (2) (InAs)⁺, 168 (5) (ClAsC_4H_9)⁺, 150 (10) (InCl)⁺, 115 (8) (In)⁺, 75 (3) (As)⁺, 57 (96) (C_4H_9)⁺.

[Li(THF)₄]₂[$(\text{InCl})_4(\text{InCl}_2)_2(\text{As}^{\text{t}}\text{Bu})_6$] (2): 1.22 g (5.5 mmol) InCl_3 were suspended in 50 mL of Et_2O at –78 °C and 0.8 g (5.5 mmol) of $\text{Li}_2\text{As}^{\text{t}}\text{Bu}$ in 20 mL of Et_2O were added under stirring. The color of the reaction mixture turned into red during the warm-up to 20 °C and a pale brown solid precipitated. The mixture was filtered and the filtrate was evaporated to dryness. The residue was dissolved in THF. After two weeks colorless needles precipitated at 20 °C.

Yield: 1.18 g (55%); m.p. 146 °C (dec.).

Elemental analysis: $\text{C}_{56}\text{H}_{118}\text{As}_6\text{Cl}_8\text{In}_6\text{Li}_2\text{O}_8$ (2355.5): calcd C 28.56, H 5.05, As 19.08, Cl 12.04, Li 0.59; found: C 28.43, H 4.92, As 19.20, Cl 11.75, Li 1.17%.

^1H NMR (CD_3CN): 1.82 ppm (m, 70 H, OCH_2CH_2 , CCH_3), 3.67 ppm (m, 16 H, OCH_2CH_3).

^{13}C NMR (CD_3CN): 26.2 ppm (OCH_2CH_2 , THF), 31.2 ppm (CCH_3 , ${}^{\text{t}}\text{BuAsIn}_2$), 34.9 ppm (CCH_3 , ${}^{\text{t}}\text{BuAsIn}_3$), 50.0 ppm (CCH_3 , ${}^{\text{t}}\text{BuAsIn}_3$), 51.4 ppm (CCH_3 , ${}^{\text{t}}\text{BuAsIn}_2$), 68.4 ppm (OCH_2CH_2 , THF).

IR (Nujol, cm^{-1}): 2722 w, 2670 w, 1630 w, 1603 m, 1312 w, 1262 m, 1209 m, 1179 m, 1150 m, 1040 s, 938 m, 914 m, 887 s, 881 s (sh), 754 m, 694 w, 675 w, 608 w, 559 w, 514 m, 465 m, 397 m, 316 s (νInCl), 281 m (sh, νInCl_2), 247 m (sh), 225 m (sh), 209 m ($\nu\text{In}_2\text{As}_2$), 153 w.

EI MS (70 eV), m/z (rel. Int. in %): 300 (12) (ClInAs_2)⁺, 150 (7) (InCl)⁺, 115 (12) (In)⁺, 75 (2) (As)⁺, 57 (43) (C_4H_9)⁺.

Table 1 Crystal data, data collection and refinement parameters

	[1]₂	2	3 · THF	4
formula	C ₁₆ H ₃₆ Cl ₄ As ₂ In ₂	C ₅₆ H ₁₁₈ As ₆ Cl ₈ In ₆ Li ₂ O ₈	C ₅₂ H ₁₀₈ As ₄ Cl ₁₂ Ga ₆ Li ₂ O ₉	C ₂₄ H ₂₀ P ₂
M _r	749.75	2355.50	2034.75	370.37
crystal size/mm	0.22 × 0.22 × 0.12	0.15 × 0.15 × 0.077	0.3 × 0.44 × 0.22	0.3 × 0.23 × 0.04
a/pm	874.2(1)	1471.7(1)	1267.0(1)	1252.2(1)
b/pm	1173.1(1)	1551.4(1)	2321.7(2)	588.7(1)
c/pm	1324.3(1)	2033.3(2)	2829.3(3)	1305.7(1)
β/°	95.35(1)	108.32(1)	90.77(1)	94.56(1)
V/pm ³ × 10 ⁶	1352.2(3)	4407.1(6)	8322(1)	959.5(2)
space group	I2/m	P2 ₁ /n	P2 ₁ /n	P2 ₁ /n
No. [47]	12	14	14	14
Z	2	2	4	2
ρ _{calc} /g cm ⁻³	1.841	1.775	1.624	1.282
T/K	190	190	190	190
abs. corr.	numerical	numerical	numerical	numerical
μ _{MoKα} /cm ⁻¹	45.3	40.6	39.2	2.3
2θ _{max} /°	51.82	51.77	52.0	51.8
h, k, l	-10 ≤ h ≤ 10 -14 ≤ k ≤ 14 -16 ≤ l ≤ 16	-17 ≤ h ≤ 15 -18 ≤ k ≤ 15 -24 ≤ l ≤ 24	-15 ≤ h ≤ 15 -28 ≤ k ≤ 28 -34 ≤ l ≤ 34	-15 ≤ h ≤ 15 -7 ≤ k ≤ 7 -16 ≤ l ≤ 14
measured refl.	5329	34321	62991	6089
unique refl.	1384	8488	16175	1835
R _{int}	0.0364	0.0552	0.0849	0.062
refl. F _o > 4σ(F _o)	1205	5839	7326	1119
parameters	61	398	794	119
R ₁ ^{a)}	0.0594	0.0372	0.0469	0.0502
wR ₂ ^{b)} (all data)	0.1868 ^{c)}	0.0834 ^{d)}	0.0904 ^{e)}	0.1292 ^{f)}
max./min. residue	1.43/-1.02	0.95/-0.47	0.59/-0.43	0.92/-0.27
electron density/epm ⁻³ × 10 ⁶				

^{a)} R₁ = Σ|F_o| - |F_c| / Σ|F_o|. ^{b)} wR₂ = [Σw(F_o² - F_c²)² / Σw(F_o²)²]^{1/2}. ^{c)} w = 1/[σ²(F_o²) + (0.0982 · P)² + 70.16 · P] and P = [max(F_o², 0) + 2 F_c²] / 3. ^{d)} w = 1/[σ²(F_o²) + (0.0456 · P)²]. ^{e)} w = 1/[σ²(F_o²) + (0.039 · P)²]. ^{f)} w = 1/[σ²(F_o²) + (0.0759 · P)²].

[Li(THF)₄]₂[(GaCl₂)₆(As^tBu)₄] · THF (3 · THF): 1.33 g (9.1 mmol) of Li₂As^tBu in 30 mL of Et₂O were added dropwise to 2.42 g (13.7 mmol) of GaCl₃ in 20 mL Et₂O at -78 °C. The yellow reaction mixture was warmed up to 20 °C and evaporated to dryness. The residue was suspended in toluene/THF, filtered and stored at 20 °C. Colorless crystals precipitated after three days. Yields: 3.09 g (67%); m.p. 136 °C (dec.).

Elemental analysis: C₅₂H₁₀₈As₄Cl₁₂Ga₆Li₂O₉ (2034.75); calcd C 30.7, H 5.35, Ga 20.56, As 14.73, Li 0.68, Cl 20.91; found C 30.45, H 5.21, Ga 21.03, As 14.74, Li 0.64, Cl 21.31%.

¹H NMR (CD₃CN): 1.92 ppm (s, 36 H, CCH₃), 1.95 ppm (s, 20 H, OCH₂CH₂, THF), 3.76 ppm (s, 20 H, OCH₂CH₂, THF).

¹³C NMR (CD₃CN): 24.9 ppm (OCH₂CH₂, THF), 34.2 ppm (CCH₃), 50.8 ppm (CCH₃), 67.1 ppm (OCH₂CH₂, THF).

IR (Nujol, cm⁻¹): 2726 w, 1345 s, 1307 m, 1294 m, 1261 m, 1153 m, 1079 s, 1042 s, 918 m, 803 w, 669 m, 584 m, 516 w, 485 m, 450 m, 435 m, 390 m, 378 m, 331 s (νGaCl₂), 295 s (νGaCl₂), 247 s (νGa₆As₄), 224 m, 191 m, 140 m, 112 m.

EI MS (70 eV), m/z (rel. Int. in %): 300 (6) [Ga₂As(C₄H₉)₂]⁺, 283 (2) (Ga₂Cl₂As)⁺, 208 (20) (Ga₂Cl₂)⁺, 174 (3) (GaCl₃)⁺, 139 (15) (GaCl₂)⁺, 133 (1) (HGaC₄H₉)⁺, 75 (1) (As)⁺, 72 (25) (THF)⁺, 69 (3) (Ga)⁺, 57 (12) (C₄H₉)⁺.

Ph₂P-PPh₂ (4): A suspension of 0.8 g (4.22 mmol) LiPPh₂ in 50 mL of toluene was added dropwise to 0.65 g (2.11 mmol) of TiCl₃ in toluene at 20 °C. A colorless solid precipitated. The mixture was stirred for 3 h at 20 °C and then filtered. The filtrate was evaporated to 5 mL. Tiny needles of **4** precipitated after one month. Yield: 0.35 g (45%); m.p. 80 °C.

Elemental analysis: C₂₄H₂₀P₂ (370.37); calcd C 77.83, H 5.44, P 16.73; found C 77.6, H 5.31, P 16.61%.

¹H NMR (C₆D₆): 6.9–8.0 ppm (m, phenyl-H).

¹³C NMR (C₆D₆): 127.2 ppm (d, ³J(PC) = 9.1 Hz, C^{3/5}), 130.0 ppm (d, ¹J(PC) = 10.1 Hz, C¹), 133.4 ppm (s, C⁴), 133.5 ppm (d, ²J(PC) = 25.7 Hz, C^{2/6}).

³¹P NMR (C₆D₆): -13.6 ppm.

IR (Nujol, cm⁻¹): 2722 w, 2667 w, 2335 w, 1953 w, 1880 w, 1807 w, 1655 w, 1583 w, 1567 m, 1330 m, 1304 m, 1260 m, 1178 m, 1159 m, 1088 m, 1067 vw, 1022 m, 997 m, 962 w, 917 w, 864 m, 848 m, 796 m, 689 m, 550 w, 526 w, 514 w, 495 s, 457 m, 438 w, 415 w, 392 m, 308 w, 249 w, 221 w.

EI MS (70 eV), m/z (rel. Int. in %): 370 (22) M⁺, 216 (1) (M-2Ph)⁺, 185 (33) (M/2)⁺, 108 (100) (PPPh)⁺, 77 (17) (Ph)⁺.

[As(As^tBu)₃]₂ (5): A solution 1.5 g (4.5 mmol) of TiCl₃ in 50 ml of THF was added to 1.34 g (4.8 mmol) of ^tBuAs(SiMe₃)₂ in 10 mL of THF. The color of the reaction mixture turned to yellow and a solid precipitated. The mixture was filtered and the filtrate was stored at 5 °C. Colorless needles of **5** precipitated during one week. Yield: 0.32 g (56%, based on ^tBuAs(SiMe₃)₂); m.p. 117 °C.

Elemental analysis: C₂₄H₅₄As₈ (942.05); calcd C 30.60, H 5.78, As 63.62; found C 30.90, H 5.94, P 64.00%.

¹H NMR (C₆D₆): 1.37 ppm (s, 9 H, CCH₃), 1.38 ppm (s, 18 H, CCH₃).

¹³C NMR (C₆D₆): 29.9 ppm (3 C, CCH₃), 30.8 ppm (6 C, CCH₃), 47.4 ppm (1 C, CCH₃), 50.9 ppm (2 C, CCH₃).

IR (Nujol, cm⁻¹): 2708 w, 1361 m, 1260 m, 1157 s, 1073 m, 1011 m, 892 m (br), 803 s, 621 w, 519 w, 391 m, 347 m, 290 m, 224 m, 150 w.

EI MS (70 eV), m/z (rel. Int. in %): 885 (13) [M-(C₄H₉)₂]⁺, 471 (29) [As₄(C₄H₉)₃]⁺, 415 (57) [HAs₄(C₄H₉)₂]⁺, 300 (23) (As₄)⁺, 75 (9) (As)⁺, 57 (100) (C₄H₉)⁺.

X-ray structure analyses of [1]₂–4: The crystals were covered with a high boiling paraffin oil and mounted on the top of a glass capillary under a flow of cold gaseous nitrogen. The orientation matrix and preliminary unit cell dimensions were determined from 2000 reflections with a IPDS system (Stoe;

Table 2 Selected bond lengths/pm and angles/ $^{\circ}$ in **[1]₂**, **2**, **3 · THF** and **4**

[1]₂			
In1–As1	265.2(1)	As1–In1–As1 a	89.95(4)
In1–Cl1	245.4(2)	In1–As1–In1 a	90.05(5)
In1–Cl2	245.9(2)	As1–In1–Cl1	115.98(5)
As1–C1	201(1)	As1–In1–Cl2	115.04(5)
		Cl1–In1–Cl2	104.99(9)
		C1–As1–C1 a	115.1(5)
2			
In1–As1	258.29(8)	As1–In1–As2	125.40(3)
In1–As2	267.58(8)	As1–In1–As3	115.94(3)
In1–As3	266.42(7)	As2–In1–As3	88.63(2)
In1–Cl1	250.3(4)	As2–In2–As3 a	107.40(3)
In2–As2	260.21(8)	As2–In3–As3	88.30(2)
In2–Cl2	247.6(4)	As2–In2–As1 a	115.26(3)
In2–Cl3	246.8(6)	As3–In3–As1 a	126.43(3)
In2–As3 a	259.63(8)	In1–As1–In3 a	97.17(3)
In3–As2	267.26(8)	In1–As2–In3	91.13(2)
In3–As3	268.29(8)	In2–As2–In3	107.25(3)
In3–Cl4	250.1(4)	In1–As3–In3	91.16(2)
In3–As1 a	258.86(8)	In1–As3–In2 a	106.86(3)
		In3–As3–In2 a	114.78(3)
3 · THF			
Ga1–As1	244.1(1)	As1–Ga1–As2	110.09(4)
Ga1–As2	244.0(1)	As1–Ga2–As3	109.63(4)
Ga2–As1	244.5(1)	As1–Ga3–As4	108.09(3)
Ga2–As3	244.4(1)	As2–Ga4–As3	109.74(4)
Ga3–As1	244.57(9)	As3–Ga5–As4	110.43(4)
Ga3–As4	244.7(1)	As2–Ga6–As4	109.67(4)
Ga4–As2	243.91(9)	Ga2–As3–Ga4	109.65(4)
Ga4–As3	244.7(1)	Ga2–As3–Ga5	107.30(4)
Ga5–As3	244.4(1)	Ga4–As3–Ga5	109.95(4)
Ga5–As4	244.0(1)	Ga3–As4–Ga5	110.63(4)
Ga6–As2	243.4(1)	Ga3–As4–Ga6	110.27(4)
Ga6–As4	243.3(1)	Ga5–As4–Ga6	108.06(4)
4			
P1–P1 a	221.7(1)	C1–P1–C2	98.3(1)
P1–C1	184.3(3)	C1–P1–P1 a	100.9(1)
P1–C2	185.8(3)	C2–P1–P1 a	99.1(1)
		P1–C1–C11	127.0(2)
		P1–C1–C15	115.1(2)
		P1–C2–C21	118.2(2)
		P1–C2–C25	122.7(2)

graphite-monochromated MoK α radiation, $\lambda = 71.073$ pm). The final cell parameters were determined with 5000 reflections. The intensities were corrected for Lorentz and polarization effects (for cell parameters and intensity collection see Table 1). The structures were solved by direct methods with the programs SHELXTL-Plus [44] (**[1]₂**, **2**, **4**) and SHELXTL [45] (**3 · THF**). The positions of the hydrogen atoms were calculated for ideal positions and refined with a common displacement parameter. Two THF molecules in **3** and one in **3 · THF** are disordered. In **2** six split positions (C521, C522; C571, C572; C641, C642; occupation factor: 0.5) and in **3 · THF** two split positions (C831, C832; occupation factors: 0.6, 0.4) could be refined.

The calculation of the bond lengths, bond angles and U_{eq} was performed by the program PLATON [46]. Further details of the crystal structure investigations may be obtained from the Fachinformationsdienst Karlsruhe, D-76344 Eggenstein-Leopoldshafen (Germany) on quoting the depository numbers CSD-410516 (**[1]₂**), CSD-410517 (**2**), CSD-410518 (**3 · THF**) and CSD-410519 (**4**).

Acknowledgement: We thank the Fonds der Chemischen Industrie for financial support.

References

- [1] A. H. Cowley, R. A. Jones, *Angew. Chem.* **1989**, *101*, 1235; *Angew. Chem. Int. Ed. Engl.* **1989**, *28*, 1208.
- [2] A. H. Cowley, *J. Organomet. Chem.* **1990**, *400*, 71.
- [3] *Chemistry of Aluminium, Gallium, Indium and Thallium*, A. J. Downs (ed.), Blackie Academic and Professionals, London, 1993.
- [4] A. H. Cowley, R. A. Jones, M. A. Mardones, J. L. Atwood, S. G. Bott, *Angew. Chem.* **1990**, *102*, 1504; *Angew. Chem. Int. Ed. Engl.* **1990**, *29*, 1409.
- [5] H. Hope, D. C. Pestana, P. P. Power, *Angew. Chem.* **1991**, *103*, 726; *Angew. Chem. Int. Ed. Engl.* **1991**, *30*, 691.
- [6] K. M. Waggoner, S. Parkin, D. C. Pestana, H. Hope, P. P. Power, *J. Am. Chem. Soc.* **1991**, *113*, 3597.

- [7] D. A. Atwood, A. H. Cowley, R. A. Jones, M. A. Mardones, *J. Am. Chem. Soc.* **1991**, *113*, 7050.
- [8] A. H. Cowley, R. A. Jones, M. A. Mardones, J. L. Atwood, S. G. Bott, *Angew. Chem.* **1991**, *103*, 1163; *Angew. Chem. Int. Ed. Engl.* **1991**, *30*, 1141.
- [9] M. B. Power, A. R. Barron, *Angew. Chem.* **1991**, *103*, 1403; *Angew. Chem. Int. Ed. Engl.* **1991**, *30*, 1353.
- [10] D. A. Atwood, A. H. Cowley, R. A. Jones, M. A. Mardones, *J. Organomet. Chem.* **1993**, *449*, C1.
- [11] M. A. Petrie, P. P. Power, *Organometallics* **1993**, *12*, 1592.
- [12] K. Niediek, B. Neumüller, *Chem. Ber.* **1994**, *127*, 67.
- [13] K. Niediek, B. Neumüller, *Z. Anorg. Allg. Chem.* **1995**, *621*, 889.
- [14] T. Belgardt, H. W. Roesky, M. Noltemeyer, H.-G. Schmidt, *Angew. Chem.* **1993**, *105*, 1101; *Angew. Chem. Int. Ed. Engl.* **1993**, *32*, 1056.
- [15] T. Belgardt, S. D. Waezsada, H. W. Roesky, H. Gorntzka, L. Häming, D. Stalke, *Inorg. Chem.* **1994**, *33*, 6247.
- [16] U. App, K. Z. Merzweiler, *Z. Anorg. Allg. Chem.* **1995**, *621*, 1731.
- [17] B. Werner, B. Neumüller, *Organometallics* **1996**, *15*, 4258 and references therein.
- [18] R. L. Wells, A. P. Purdy, A. T. McPhail, C. G. Pitt, *J. Chem. Soc., Chem. Commun.* **1986**, 487.
- [19] M. Driess, K. Merz, H. Pritzkow, R. Janoschek, *Angew. Chem.* **1996**, *108*, 2688; *Angew. Chem. Int. Ed. Engl.* **1996**, *35*, 2507.
- [20] M. Driess, S. Kuntz, K. Merz, H. Pritzkow, *Chem. Eur. J.* **1998**, *4*, 1628.
- [21] R. L. Wells, A. P. Purdy, A. T. McPhail, C. G. Pitt, *J. Organomet. Chem.* **1988**, *354*, 287.
- [22] J. D. Johansen, A. T. McPhail, R. L. Wells, *Advanced Materials for Optics and Electronics* **1992**, *1*, 29.
- [23] A. Dashti-Mommertz, B. Werner, B. Neumüller, *Polyhedron* **1998**, *17*, 523 and references therein.
- [24] C. von Hänisch, D. Fenske, *Z. Anorg. Allg. Chem.* **1997**, *623*, 1040.
- [25] S. Berger, S. Braun, H.-O. Kalinowski, *NMR-Spektroskopie von Nichtmetallen*, Vol. 3, ^{31}P -NMR-Spektroskopie, Thieme Verlag, Stuttgart, 1993.
- [26] S. Aime, R. K. Harris, E. M. McVicker, M. Fild, *J. Chem. Soc., Dalton Trans.* **1976**, 2144.
- [27] A. H. Cowley, R. A. Jones, K. B. Kidd, C. M. Nunn, D. L. Westmoreland, *J. Organomet. Chem.* **1988**, *341*, C1.
- [28] a) B. Neumüller, *Z. Naturforsch.* **1990**, *45 b*, 1559; b) B. Neumüller, *Z. Naturforsch.* **1991**, *46 b*, 753; c) B. Neumüller, *Z. Naturforsch.* **1991**, *46 b*, 1539 and references therein.
- [29] a) G. Fritz, *Angew. Chem.* **1987**, *99*, 1150; *Angew. Chem. Int. Ed. Engl.* **1987**, *26*, 1111; b) G. Sawitzki, H.-G. von Schnering, *Z. Anorg. Allg. Chem.* **1973**, *399*, 257; c) G. Fritz, H. J. Dannagel, E. Matern, *Z. Anorg. Allg. Chem.* **1973**, *399*, 263.
- [30] T. Hascall, K. Ruhlandt-Senge, P. P. Power, *Angew. Chem.* **1994**, *106*, 350; *Angew. Chem. Int. Ed. Engl.* **1994**, *33*, 356.
- [31] S. Anfang, G. Seyberth, K. Harms, G. Geiseler, W. Massa, K. Dehnicke, *Z. Anorg. Allg. Chem.* **1998**, *624*, 1187.
- [32] M. B. Power, J. W. Ziller, A. R. Barron, *Organometallics* **1992**, *11*, 2783.
- [33] A. Boardman, R. W. H. Small, I. J. Worrall, *Inorg. Chim. Acta* **1986**, *120*, L23.
- [34] A. F. Wells, *Structural Inorganic Chemistry*, 5th ed., Clarendon Press, Oxford, 1990.
- [35] K. T. Higa, C. George, *Organometallics* **1990**, *9*, 275.
- [36] M. A. Petrie, P. P. Power, *J. Chem. Soc., Dalton Trans.* **1993**, 1737.
- [37] A. P. Purdy, R. L. Wells, A. T. McPhail, C. G. Pitt, *Organometallics* **1987**, *6*, 2099.
- [38] a) O. Mundt, H. Riffel, G. Becker, A. Simon, *Z. Naturforsch.* **1988**, *43 b*, 952 and references therein; b) S. G. Baxter, A. H. Cowley, R. E. Davis, P. E. Riley, *J. Am. Chem. Soc.* **1981**, *103*, 1699; c) R. Richter, J. Kaiser, J. Sieler, H. Hartung, C. Peter, *Acta Cryst.* **1977**, *33 b*, 1887; d) G. Fritz, H. Goesmann, B. Mayer, *Z. Anorg. Allg. Chem.* **1992**, *607*, 26; e) F. Knoch, R. Appel, B. Bruck, *Z. Kristallogr.* **1995**, *210*, 1995; f) R. Heinicke, R. Kadyrov, *J. Organomet. Chem.* **1996**, *520*, 131.
- [39] O. Mundt, H. Riffel, G. Becker, A. Simon, *Z. Naturforsch.* **1984**, *39 b*, 317 and references therein.
- [40] D. D. Perrin, W. L. F. Armarego, D. R. Perrin, *Purification of Laboratory Chemicals*, 2nd ed., Pergamon Press, Oxford, 1980.
- [41] H. Schmidbaur in: *Handbuch der Präparativen Anorganischen Chemie*, Vol. II, 3rd ed., Ferdinand Enke Verlag, Stuttgart, 1978.
- [42] E. W. Wartenberg, J. Goubeau, *Z. Anorg. Allg. Chem.* **1964**, *329*, 269.
- [43] LiPPh₂, LiAs^tBu₂ and Li₂As^tBu were prepared according: K. Niediek, B. Neumüller, *Z. Anorg. Allg. Chem.* **1993**, *619*, 885.
- [44] G. M. Sheldrick, SHELLXTL-Plus, Release 4.2 for Siemens R3 Crystallographic Systems, Siemens Analytical X-Ray Instruments Inc., Madison (WI), 1990.
- [45] G. M. Sheldrick, SHELLXTL, Release 5.05/VMS for Siemens R3 Crystallographic Research Systems, Siemens Analytical X-Ray Instruments Inc., Madison (WI), 1996.
- [46] A. L. Spek, *PLATON-94*, Utrecht, 1994.
- [47] *International Tables for Crystallography*, 2nd ed., Vol. A, Kluwer Academic Publishers, Dordrecht, **1989**.